UCRL-75044
PREPRINT
Conf-740202--1

LAWRENCE LIVERMORE LABORATORY
University of California/Livermore, California

IN-PLACE LEACHING OF PRIMARY SULFIDE ORES: LABORATORY LEACHING DATA AND KINETICS MODEL

R. L. Braun
A. E. Lewis
M. E. Wadsworth

October 31, 1973

This paper was prepared for presentation at the AIME Solution Mining Symposium, Dallas, February 1974, and for subsequent publication in the symposium proceedings.

IN-PLACE LEACHING OF PRIMARY SULFIDE ORES: LABORATORY LEACHING DATA AND KINETICS MODEL*

R. L. Braun, A. E. Lewis, and M. E. Wadsworth†

Lawrence Livermore Laboratory, University of California
Livermore, California 94550

ABSTRACT

Experimental results obtained in laboratory leaching studies of primary copper sulfide ore in sulfuric acid systems pressurized with oxygen are interpreted by a computerized geometric model involving the movement of a reaction zone through the ore fragments. Physical properties of the ore, including size, shape, and mineral content, are considered. The leaching mechanism involves mixed kinetics and includes a surface reaction within a moving reaction zone plus pore diffusion of dissolved oxygen through the reacted portion of the ore fragment to the reaction zone. The results are applicable to conditions that would exist in nuclear solution mining or similar processes in which the ore is converted into rubble and then inundated by a leach solution adequately supplied with oxidants. Experimental results at 90°C are correlated with the model, which includes temperature-dependent parameters.

INTRODUCTION

A concept for the in situ leaching of copper ores containing chalcopyrite has been described (1,2,3). The first step is rubblization in place by some suitable method, such as the use of nuclear explosives or undercutting and caving—possibly assisted by conventional explosives. The ore fragments are then leached in the

*Work performed under the auspices of the U. S. Atomic Energy Commission.

†University of Utah, Salt Lake City, Utah.

aqueous, sulfuric acid system produced by introducing oxygen into the flooded ore under a hydrostatic pressure. The increase in solubility of the oxygen under these conditions, as well as the increase in temperature that is attainable, greatly accelerates the rate of copper recovery from primary copper ores, in which most of the copper occurs as chalcopyrite.

Experimental and theoretical work has been conducted at the Lawrence Livermore Laboratory during the past few years on the leaching of chalcopyrite ores. The objective of this work is to obtain experimental data and to develop a theory that will enable extrapolation of results from laboratory conditions and scale to field conditions and scale. An understanding of the effect of particle size distribution, temperature, acid concentration, mineralogy, etc. on the rate of recovery are essential to successful operation of this process.

In this paper we will present some of the experimental data and a model that we believe successfully describes the recovery of copper from ore fragments of any given particle size distribution under limited conditions of temperature and pH. An easy application of the model to higher temperatures and acid concentrations is difficult because of replacement reactions between copper in solution and chalcopyrite within ore fragments, as well as other changes in the chemistry of the system at low pH. Some of these will be the subject of later papers.

EXPERIMENTAL

Equipment

Leaching experiments were conducted in autoclaves ranging in capacity from 0.5 l to 3800 l. The largest system is shown schematically in figure 1. The vessel is made of type A-36 steel and is integrally lined with 5/32-in. chemical lead. The liner is treated with dilute H_2SO_4 to provide a layer of $PbSO_4$ and thus eliminate further interaction with H_2SO_4 produced during the leaching phase. The sampling probes, thermocouple sheaths, and oxygen inlet pipe are made of Carpenter-20 stainless steel. The temperature of the solution within the autoclave is maintained to within ±2°C of the desired operating temperature by external electrical heater tapes beneath the insulation. The gas inlet pressure is regulated, and the flow of gas through the system is controlled by a needle valve to give the desired flow rate as indicated by the pressure drop across a known orifice at the gas exit.

The smaller systems of capacity 0.5 l to 20 l are shown schematically in figure 2. The vessel is made of stainless steel lined with chemical lead and is heated externally. The sampling probe, thermocouple sheath, and oxygen inlet tube are made of titanium.

A Oxygen supply
B Pressure regulator
C Check valve
D Oxygen inlet
E Air-cooled condenser
F Pressure relief valve and pressure gauge
G Filter
H Needle valve
I Flowmeter
J Thermocouple
K Liquid sampling tube
L Liquid retention cylinder
M Liquid exit
N Liquid adit
O Ore level
P Liquid level

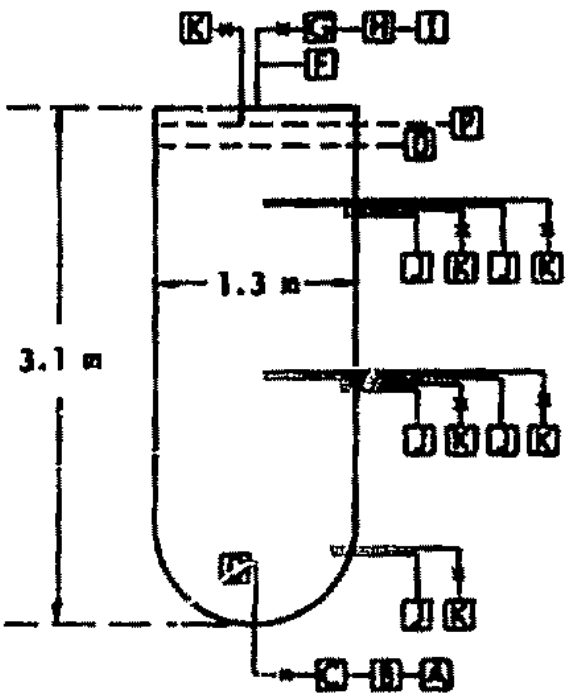

FIG. 1. - Diagram of Reactor for Experiment Exp-L1

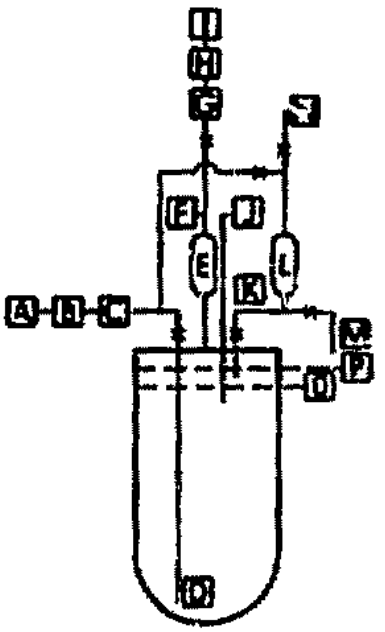

FIG. 2. - Diagram of Small Reactor

These systems have a provision for removal of liquid samples for chemical analysis during the course of the reaction without disrupting the operating temperature or pressure.

Ore Type

The ore used in these experiments is a primary porphyry copper ore from the San Manuel Mine (Magma Copper Company, Arizona). The mineral assemblage, determined by x-ray diffraction and optical microscopy, is principally quartz and sericite, with minor amounts of feldspar, chlorite, biotite, calcite, chalcopyrite, and pyrite. In addition, there are trace amounts of hematite, epidote, and hornblende—and rare occurrences of bornite, covellite, and magnetite. The chemical analysis of a composite sample is shown in table 1. A pyrite/chalcopyrite mole ratio of 2.0 is calcu-

TABLE 1. - Chemical analysis in wt% of San Manuel ore composite

Cu	0.71	Na	1.11
Fe	3.17	K	2.06
S	2.17	Ca	0.62
CO_2	0.42	Mg	0.30
Si	31.20	Al	8.10

lated from this assay. Density and communicated porosity measurements on 40 pieces of ore gave the following average values: bulk dry density = 2.57 g cm^{-3}, bulk saturated density = 2.63 g cm^{-3}, bulk grain density = 2.73 g cm^{-3}, and porosity = 0.06.

Procedure

The autoclave is hand loaded with a weighed amount of ore of known size distribution. A measured amount of deionized water is added to cover the ore. The system is pressurized with oxygen to 395 psig and heated to 90°C (giving P_{H_2O} = 10 psia and P_{O_2} = 400 psia). Flow of oxygen is then begun. Circulation of the solution within the vessel is only the convective stirring which is induced by the rise of oxygen bubbles. After a period of one day, an additional measured amount of water is added to the system to reach the final liquid levels shown in figures 1 and 2. These liquid levels are maintained for the duration of the experiment by periodically adding water to replenish both the water lost by evaporation and the solution removed by sampling. In figure 1 this is done by maintaining the level so that the liquid can just be withdrawn through the sampling probe at the top of the vessel. In figure 2 the level is maintained so that a constant amount (nominally 50 ml) of liquid can be withdrawn through the sampling system.

Periodically, samples of the pregnant liquor are taken for chemical analysis. In figure 1, 300 ml of solution are first allowed

to flush the sampling line before sampling is begun. This amount is later returned to the system by means of a Sprague injection pump. In figure 2 the sampling is done by retaining 2 ml of the 50 ml of solution withdrawn into the sampling cylinder. The amount not retained is returned to the autoclave. The small amount of copper contained in solutions not returned to the autoclave is taken into account in the data reduction. For uncompleted experiments, the copper fraction extracted is based on the assay of 0.7 wt% Cu for the composite sample of San Manuel ore. For completed experiments, the copper fraction extracted is based on a corrected assay of the ore as determined from the total amount of copper present in the leached ore, the pregnant liquor, and the retained samples.

EXPERIMENTAL RESULTS

The five leaching experiments that will be discussed have been designated Exp-L1, -L2, -L3, -L4, and -L5. Each was conducted at 90°C and at an oxygen partial pressure of 400 psia. Table 2 lists the oxygen flow rates, the quantities of solution and ore, and the grade of ore. High oxygen flow rates were used so that the measured leaching rates would not be limited by the availability of oxygen in the bulk solution, since the purpose of the experiments is to provide leaching data for near-maximum oxygen content in the bulk solution at the selected temperature and pressure.

Figure 3 shows the partial size distribution of each ore charge, determined by screening. The ore charge for Exp-L1 was a specially selected coarse size fraction of run-of-mine San Manuel Ore. The size distribution for Exp-L1 is based on recent measurements of Potter (4), superseding the earlier reported (2) estimates. The ore charges for Exp-L3 and Exp-L5 were screened samples from run-of-mill San Manuel ore. The ore charges for Exp-L2 and Exp-L4 were screened samples from large pieces of run-of-mine San Manuel ore that had undergone additional crushing in the laboratory. Although the ore particles for all five experiments deviated

TABLE 2. - Physical data for experiments

Experiment No.	Duration (days)	Oxygen flow rate (cm^3(STP)/min)	Solution volume (cm^3)	Ore weight (g)	Ore grade (wt fraction $CuFeS_2$)
Exp-L1	[a]717	[b]1.2×10^4	1.42×10^6	5.8×10^6	0.020
Exp-L2	[a]468	480	9.03×10^3	2.45×10^4	0.020
Exp-L3	154	160	250	248	0.017
Exp-L4	180	160	284	250	0.020
Exp-L5	96	160	250	245	0.017

[a]Experiment still in progress

[b]Flow rate for Exp-L1 was 2.4×10^4 cm^3(STP)/min during first 90 days of experiment

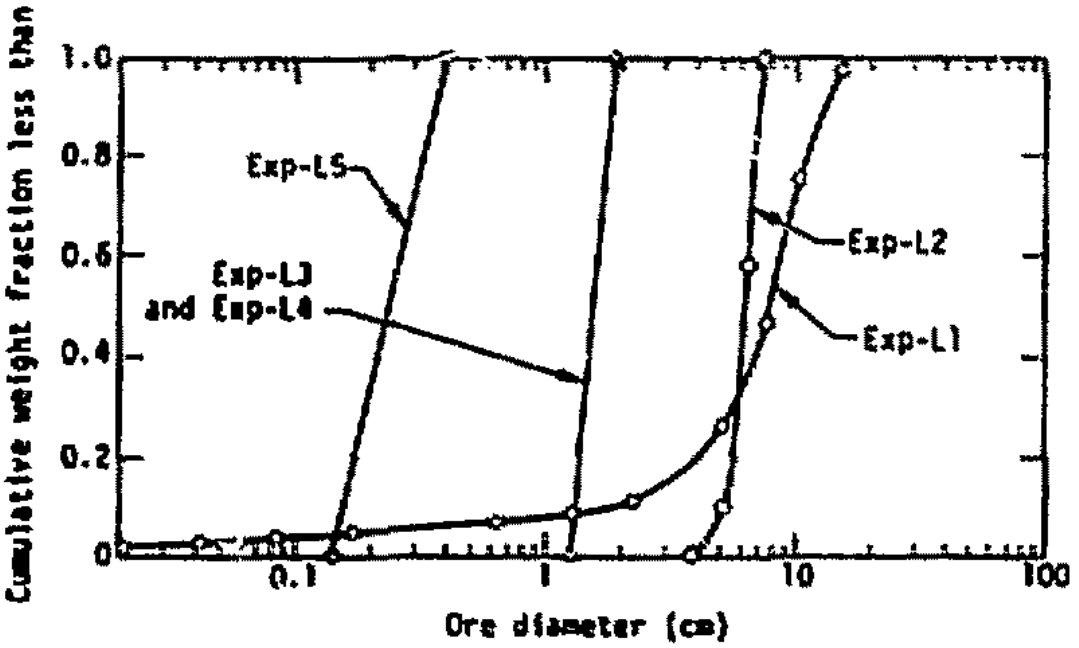

FIG. 3. - Ore Particle Size Distributions

from isometry, the particles in Exp-L1 were approximately isometric. The ore particles for Exp-L4, which were generated in a small laboratory jaw crusher, deviated most from an isometric shape. Particle shape, of course, significantly affects the leaching rate and, as will be shown later, a shape parameter ($0 < \phi_{10} \leq 1$) may be determined from the leaching data. This parameter corrects for both the particle surface roughness and the deviation of the particle shape from sphericity.

Copper leaching data (copper fraction extracted from the ore as a function of time) are shown in figure 4 for Exp-L1 and in figure 5 for the remaining experiments. The extraction curves follow the basic pattern discussed by Harris (5) for leaching low-porosity particles of ore in which the sulfide is disseminated throughout. This is particularly pronounced for the long-term leaching of large particles of ore in Exp-L1 (figure 4), where the initially high rate of copper extraction from the chalcopyrite exposed at the surface of the ore fragments is followed by a lower, diffusion-limited rate of extraction of copper from the interior of the fragments.

A rapid initial release of copper values to solution is particularly evident for Exp-L2 (figure 5). Fracturing along natural weakness planes exposes surfaces of high sulfide mineralization, which are rapidly attacked during the initial stages of leaching. This effect

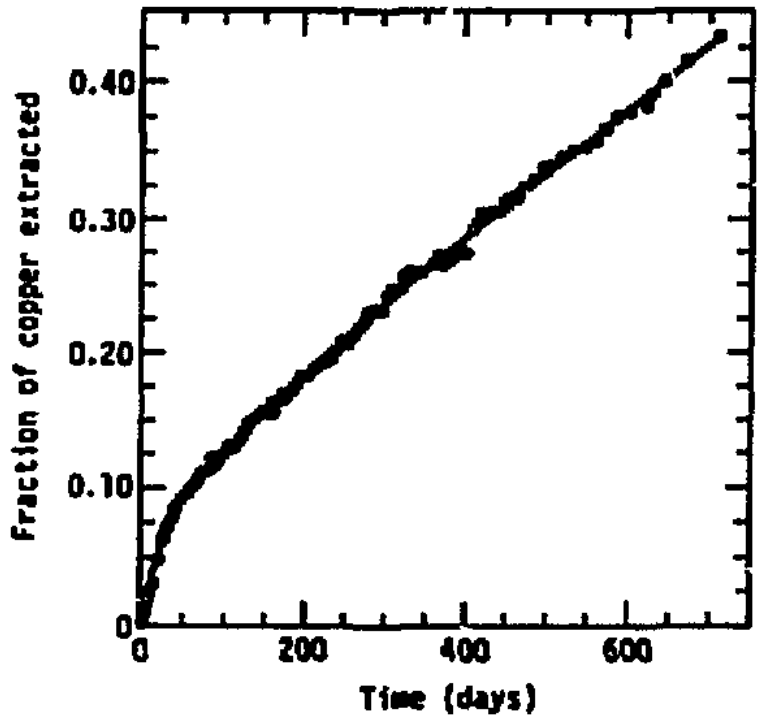

FIG. 4. - Extraction of Copper from Coarse-Sized Primary Sulfide Ore at 90°C and 400 psia Oxygen (Exp-L1)

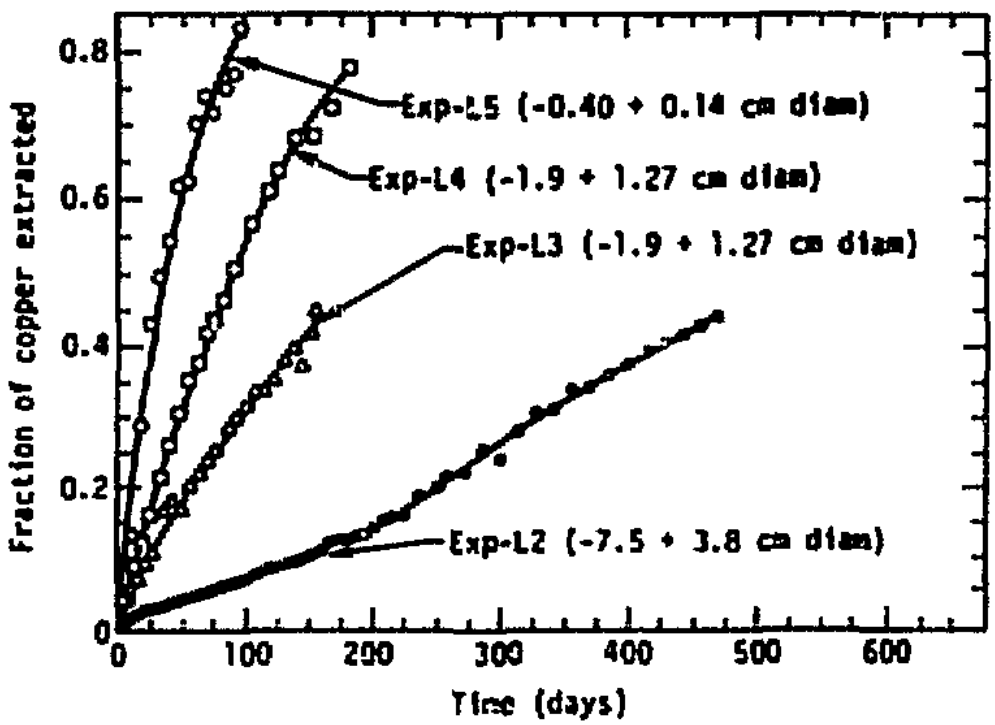

FIG. 5. - Extraction of Copper from Primary Sulfide Ore of Various Size Ranges at 90°C and 400 psia Oxygen

is less noticeable for small ore particles of average radius less than 1 cm (Exp-L3, -L4, and -L5 in figure 5) because of the rapid leaching of all contained copper, and also because fracturing across the grain structure—rather than along boundaries--becomes predominant.

The effect of particle shape on leaching rate is clearly illustrated for Exp-L3 and Exp-L4. Although both experiments utilized ore particles of the same screened size range, the flatter aspect of the particles in Exp-L4 caused a pronounced increase in the measured leaching rate.

Before interpreting the leaching data, the chemical reactions occurring during leaching will be considered. In each of the experiments just discussed, the pH of the leach solution (measured at 25°C) decreased from an initial value of 5.5 to a steady-state value near 2. This is illustrated for Exp-L1 in figure 6. Acid-generating reactions caused the pH to decrease rapidly to 1.7 during the first 60 days. Thereafter, the pH increased slightly to 1.9, where it has remained for the duration of the experiment. This buffering effect is an important feature of the leaching system and represents a steady-state balance of H^+-dependent reactions involving both the sulfides and gangue constituents.

The important buffering reactions associated with the dissolution of chalcopyrite and pyrite are:

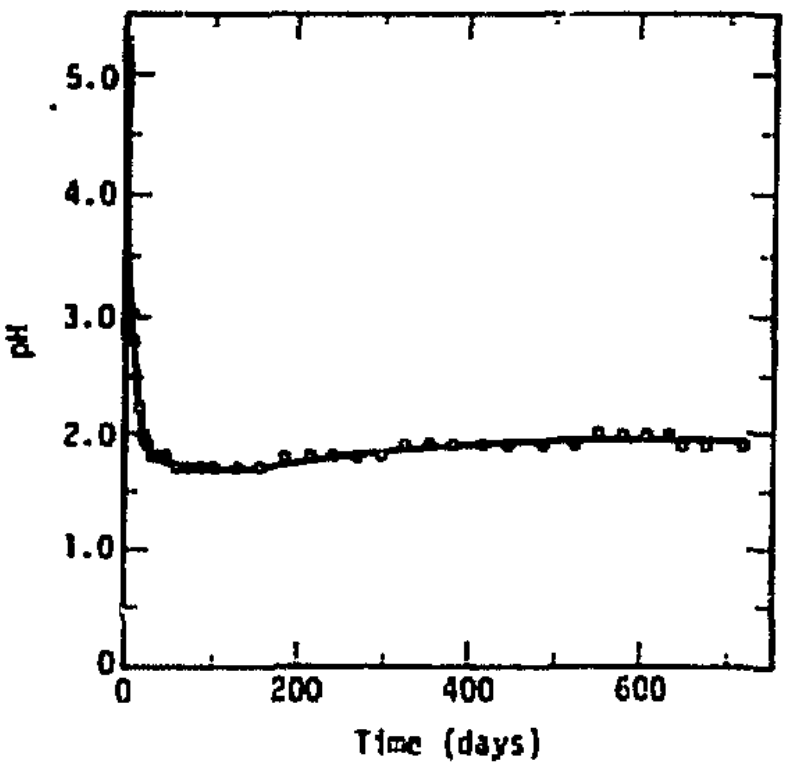

FIG. 6. - pH of Pregnant Liquor During Leach of Coarse-Sized Primary Sulfide Ore (Exp-L1)

Acid-consuming reactions:

$$CuFeS_2 + \frac{5}{4}O_2 + 5H^+ = Cu^{+2} + Fe^{+3} + 2S^\circ + \frac{5}{2}H_2O \quad (1)$$

$$FeS_2 + \frac{3}{4}O_2 + 3H^+ = Fe^{+3} + 2S^\circ + \frac{3}{2}H_2O \quad (2)$$

$$CaCO_3 + 2H^+ + SO_4^{-2} = CaSO_4 + CO_2 + H_2O \quad (3)$$

(Acid-consuming reactions involving other gangue constituents will be discussed later).

Acid-generating reactions:

$$S^\circ + \frac{3}{2}O_2 + H_2O = 2H^+ + SO_4^{-2} \quad (4)$$

$$Fe^{+3} + \frac{3}{2}H_2O = 3H^+ + \frac{1}{2}Fe_2O_3 \quad (5)$$

$$Fe^{+3} + \frac{7}{3}H_2O + \frac{2}{3}SO_4^{-2} = \frac{5}{3}H^+ + \frac{1}{3}Fe_3(SO_4)_2(OH)_5 \cdot 2H_2O \quad (6)$$

The hydrolysis of Fe^{+3} to form hematite or hydrogen jarosite in Eqs. (5) and (6) is an important part of the buffering capacity of the system. X-ray diffraction analysis has shown that the major iron-containing precipitate produced during the leaching of San Manuel ore at 90°C and 400 psi is hydrogen jarosite. Hematite, although readily detectable optically, is produced in much smaller quantities than the very abundant hydrogen jarosite. These observations are in agreement with the Fe^{+3} and SO_4^{-2} chemical analyses during Exp-L1. That is, the SO_4^{-2} concentration (moles/l) increased from 0.163 M at 75 days of reaction to 0.431 M at 607 days of reaction, while the Fe^{+3} concentration decreased from 0.0025 M to 0.0000 M during the same time period. This decrease in Fe^{+3} with increasing SO_4^{-2} indicates solution equilibrium with hydrogen jarosite according to Eq. (6).

The net reaction for Exp-L1 at 607 days of reaction time can then be written as:

$$CuFeS_2 + 2FeS_2 + CaCO_3 + \frac{45}{4}O_2 + \frac{37}{6}H_2O = Cu^{+2} + Fe_3(SO_4)_2(OH)_5 \cdot 2H_2O + CaSO_4 + \frac{1}{3}S^\circ + \frac{8}{3}SO_4^{-2} + \frac{10}{3}H^+ + CO_2 \quad (7)$$

In this reaction we have used the facts that the ore contains a pyrite/chalcopyrite mole ratio of 2.0 and that for an oxygen diffusion-limited reaction, the pyrite and chalcopyrite oxidation rates are approximately equal. We have also used the fact that at 607 days approximately 1 mole of $CaCO_3$ has reacted for each mole of Cu^{+2} generated, based on CO_2 evolution measurements. Further, we have neglected the quantity of iron in solution, which is small compared with the amount of iron released from the sulfide minerals and reprecipitated as hydrogen jarosite. Finally, we have written the equation so that it is consistent with the solution chemistry of the system at 607 days as shown in table 3. The equation indicates

TABLE 3. - Composition of pregnant liquor in Exp-L1 after 607 days of leaching

	Molarity (moles/l)	Normality (equivalents/l)
Cu^{+2}	0.1697	0.3394
H^{+}	0.01	0.01
Na^{+}	0.0022	0.0022
K^{+}	0.0001	0.0001
Ca^{+2}	0.0097	0.0194
Mg^{+2}	0.2217	0.4434
Al^{+3}	0.0211	0.0633
Fe^{+3}	0.0009	0.0027
SO_4^{-2}	0.4406	0.8812

that 2.67 moles of SO_4^{-2} are in solution per mole of Cu^{+2}, in agreement with the measured ratio of 2.6. Furthermore, it indicates that 3.3 moles of H^{+} are formed per mole of Cu^{+2}, again in agreement with the measurement of 3.2 equivalents of (H^{+}, Fe^{+3}, Na^{+}, K^{+}, Ca^{+2}, Mg^{+2}, and Al^{+3}) in solution per mole of Cu^{+2}. The H^{+} generated according to Eq. (7) has thus largely reacted with the gangue minerals to yield an equivalent quantity of other cations, leaving the pH constant at 1.9.

The net reaction as expressed in Eq. (7) is useful in that it gives an indirect measurement of the oxygen requirements: namely, 11.25 moles of oxygen per mole of copper for leaching an ore in which the pyrite/chalcopyrite mole ratio is 2.0 This stoichiometry number (σ = 11.25) will be used later in the copper extraction calculation.

It must be realized that σ may be different for other ores. For example, if the pyrite/chalcopyrite mole ratio were only 1, it can be shown, from a decomposition of Eq. (7), that $\sigma = 7.5$. Furthermore, if the ore contained appreciable amounts of Fe^{+2}, as in the form of biotite, the oxygen requirements would be slightly greater when leaching is done under conditions for which biotite is attacked. The latter oxygen requirement is low, however, since only 0.25 mole of oxygen per mole of Fe^{+2} is consumed.

Finally, experimental results relating to other physical and chemical changes occurring in the leaching process are presented. Figure 7 shows a cross-section of a slightly leached particle of ore, illustrating that the leaching process essentially involves an unreacted core surrounded by the reacted portion. The outer, reacted portion contains hematite and hydrogen jarosite produced by the reaction. There is no evidence from copper extraction data that the sulfide dissolution reactions are quenched by the precipitation of these iron salts. This is in agreement with measurements of the porosity of leached ore particles from Exp-L4, which revealed that the porosity remained at nearly the initial value of 0.060 during the course of leaching 80% of the copper. The deposition of iron salts, while not acting to quench the reaction, does somewhat limit access

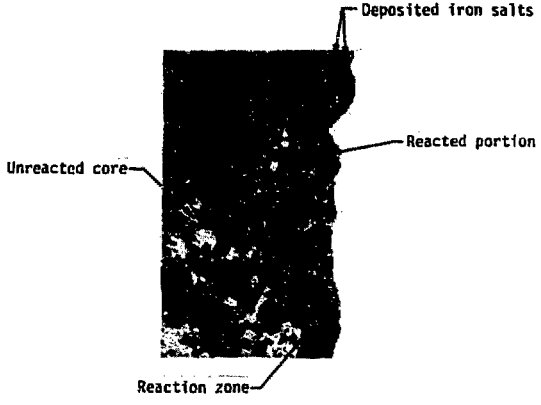

FIG. 7. - Polished Section of Partially Reacted Ore Fragment Showing Topochemical Character of the Leaching Process (photo)

of dissolved oxygen to the interior of the ore, as evidenced by increased copper dissolution rates under conditions for which iron is not as completely deposited. The latter conditions will not be considered in this report.

The copper extraction data for Exp-L1 and -L2 indicate more rapid leaching than expected after extended periods of time. This is particularly evident in figure 5 for Exp-L2, where the leaching rate actually accelerated after 150 days. Exp-L2 was interrupted after 450 days of continuous reaction. This was done to determine the physical factors accounting for the increased rate of reaction after 150 days. It was found that nonuniform penetration of the reaction zone along grain boundaries and fractures had occurred. In some cases the penetration resulted in fragmentation of the particles. The net result was an effective increase in the reaction surface, which accounts for the enhanced rates. Physical changes that occur in the ore are therefore important, though difficult, features required of a leaching model. Corrections of this type are particularly required for the larger ore fragments, which must be exposed to the solution for much longer periods of time for equivalent copper extraction.

THEORY AND DISCUSSION

The presence of a moving boundary with an essentially unreacted core suggests a reaction zone separating a core or unreacted portion from an essentially completely reacted outer region. A model similar to that proposed by Valensi (6) and Ross et al. (7) for high-temperature gas-solid reactions correlates the data well and lends itself to broad variations in geometry. Essentially, the model involves steady-state diffusion of the reactant through the previously reacted portion of the ore fragment, followed by chemical reaction within the reaction zone. The use of such a model for an ore fragment requires some detail because the leaching reaction occurs at the site of special included minerals present in veinlets or as discreet disseminated particles. Reactants and products of the leaching process must therefore be transported in solution-filled channels within the ore fragment. The model further assumes that circulation of leach solution around the particle is sufficient to maintain oxidant concentration so that bulk solution transport is not rate controlling. The kinetics are limited, then, only by processes occurring within the ore fragments.

Reaction Zone Model

The model used here is based upon spherical geometry, and deviations from a sphere will be corrected by a geometry factor, ϕ_{lo}, which includes both boundary roughness and sphericity factors. Figure 8 represents an idealized ore particle showing the reaction

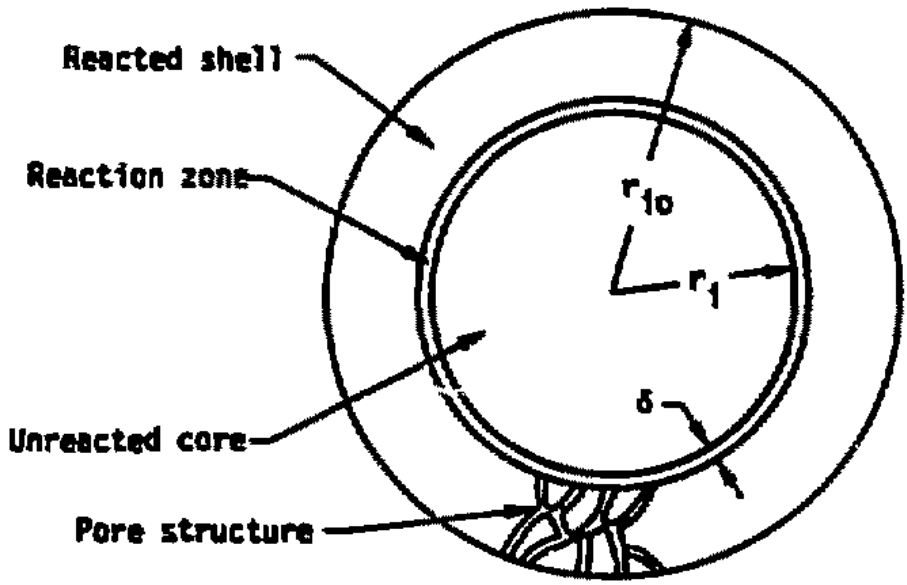

FIG. 8. - Ore Particle of Radius r_{io}, Showing Reaction Zone

zone of thickness (δ). The original average radius is r_{io} and the radius at time t is r_i.

The reaction zone may be viewed as a region in which disseminated sulfide particles are in all stages of reaction. As the zone moves to smaller values of r_i, mineral particles are included in the zone. At the trailing edge of the zone the last vestige of unreacted material disappears. This is an oversimplification, since some larger unreacted sulfide particles will remain behind. Examination of partially leached ore fragments does indicate that the majority of the sulfide particles originally present in the outer shell ($r > r_i$) have in fact reacted to completion. Within the moving reaction zone the concentration of reacting particles and the effective chemical leaching area of sulfide particles may be considered essentially constant.

The rate of reaction within the leaching zone may be expressed for a given particle by the equation

$$\left(\frac{dn}{dt}\right)_i = -\left(\frac{4\pi r_i^2}{\phi_{io}}\right) \delta n_p A_p C_i k, \qquad (8)$$

where n_p is the number of sulfide particles per unit volume of rock and A_p is the average area per sulfide particle. The concentration C_i refers to the reactant concentration in the reaction zone (in this case oxygen), k is the rate constant, and n is the number of moles of unreacted chalcopyrite in one ore fragment. Under steady-state conditions, the rate of transport to the reaction zone will equal the

rate within the reaction zone. Diffusion through pores to the reaction zone may be expressed by the equation

$$\left(\frac{dn}{dt}\right)_i = -\left(\frac{4\pi r^2}{\phi_{io}}\right)\left(\frac{Df}{\sigma}\right)\left(\frac{dC}{dr}\right) = J_i, \tag{9}$$

where D is the coefficient of diffusion for the reactant and σ is the stoichiometry number. The factor f is related to porosity and contains the fraction of surface made up of pore area. The tortuosity also is included in f.

For a given value of r_i, Eq. (9) may be integrated for steady-state conditions (J_i = constant) for all r values between r_i and r_{io}, which upon combination with Eq. (8) gives an expression for the concentration of reactant C_i in the reaction zone in terms of the bulk solution concentration C_b, or

$$C_i = C_b\left[\frac{1}{1 + \left(\frac{\delta n_p A_p \sigma k}{Df}\right)\left(\frac{r_i}{r_{io}}\right)(r_{io} - r_i)}\right]. \tag{10}$$

Substituting in Eq. (8) gives the generalized rate expression

$$\left(\frac{dn}{dt}\right)_i = \frac{4\pi r_i^2}{\phi_{io}} C_b\left[\frac{1}{\left(\frac{1}{\delta n_p A_p k}\right) + \left(\frac{\sigma}{Df}\right)\left(\frac{r_i}{r_{io}}\right)(r_{io} - r_i)}\right]. \tag{11}$$

The grade G (weight fraction copper sulfide mineral) is given by

$$G = \frac{\delta_p A_p r_p \rho_p}{3\rho_r}, \tag{12}$$

where r_p is the average spherical copper sulfide particle radius, ρ_p is the density of the copper sulfide, and ρ_r is the bulk rock density. Combining Eqs. (11) and (12) gives

$$\left(\frac{dn}{dt}\right)_i = -\frac{4\pi r_i^2}{\phi_{io}} C_b \left[\frac{1}{\left(\frac{1}{G\beta}\right) + \left(\frac{\sigma}{Dr}\right)\left(\frac{r_i}{r_{io}}\right)(r_{io} - r_i)}\right], \tag{13}$$

where

$$\beta = \frac{3\rho_r \delta k}{r_p \rho_p}. \tag{14}$$

Analytical Integration of Leaching Rate

Equation (13) applies for a given particle size (r_{io}) and is useful in integrated form for the analysis of laboratory studies on sized particles to identify kinetic models and associated parameters. It is also useful to normalize the rate in terms of fraction reacted (α), since α for a single particle or an assemblage of particles of size r_{io} is the same. For a given particle,

$$\alpha_i = 1 - \frac{r_i^3}{r_{io}^3}. \tag{15}$$

For a sample of broad particle size distribution of i sizes,

$$\alpha = \sum_i \alpha_i W_i, \tag{16}$$

where α_i is the fraction reacted for size r_{io} and W_i is the weight fraction of that size.

The number of moles of unreacted mineral in the core of the particle is given by

$$n = \frac{4}{3} \frac{\pi r_i^3 \rho_r G}{M}, \tag{17}$$

where M is the molecular weight of the copper sulfide mineral. The rate of movement of the reaction interface may be determined from Eqs. (13) and (17):

$$\left(\frac{dr_i}{dt}\right) = -\frac{M\,C_b}{\phi_{io}\,\rho_r\,G}\left[\frac{1}{\left(\frac{1}{G\beta}\right) + \left(\frac{\sigma}{Df}\right)\left(\frac{r_i}{r_{io}}\right)(r_{io} - r_i)}\right]. \tag{18}$$

The fractional reaction rate ($d\alpha/dt$) may be determined from Eqs. (15) and (18) such that

$$\frac{d\alpha}{dt} = \frac{3MC_b}{\phi_{io}\,\rho_r\,G\,r_{io}}\left\{\frac{(1-\alpha)^{2/3}}{\left(\frac{1}{G\beta}\right) + \left(\frac{\sigma\,r_{io}}{Df}\right)(1-\alpha)^{1/3}\left[1-(1-\alpha)^{1/3}\right]}\right\}. \tag{19}$$

In integrated form, Eq. (19) becomes

$$1 - \frac{2}{3}\alpha - (1-\alpha)^{2/3} + \frac{\beta'}{Gr_{io}}\left[1-(1-\alpha)^{1/3}\right] = \frac{\gamma}{\phi_{io}Gr_{io}^2}\,t, \tag{20}$$

where

$$\beta' = \frac{2Dfr_p\rho_p}{3\sigma\rho_r\delta k} = \frac{2Df}{c\beta} \tag{21}$$

and

$$\gamma = \frac{2MDfC_b}{\rho_r\sigma}. \tag{22}$$

Copper extraction curves can now be calculated by Eq. (20) when the ore particle size range is narrow enough to be described adequately by one average size. This is shown in figure 9 for Exp-L2, -L3, -L4, and -L5, for which $\bar{r}_{io}$ = 3.0, 0.8, 0.8, and 0.15, respectively. In each calculation, empirically determined values of β' = 0.0121 cm and $\gamma = 7.59 \times 10^{-11}$ cm^2 sec^{-1} were used. Because of the differences in ore particle geometry among the several experiments, as described earlier, no single value of the shape factor (ϕ_{io}) can be used. Therefore, ϕ_{io} = 0.52 was used for Exp-L3, based on computer evaluation of the rate parameters (to be described later). The ϕ_{io} values for the other experiments were

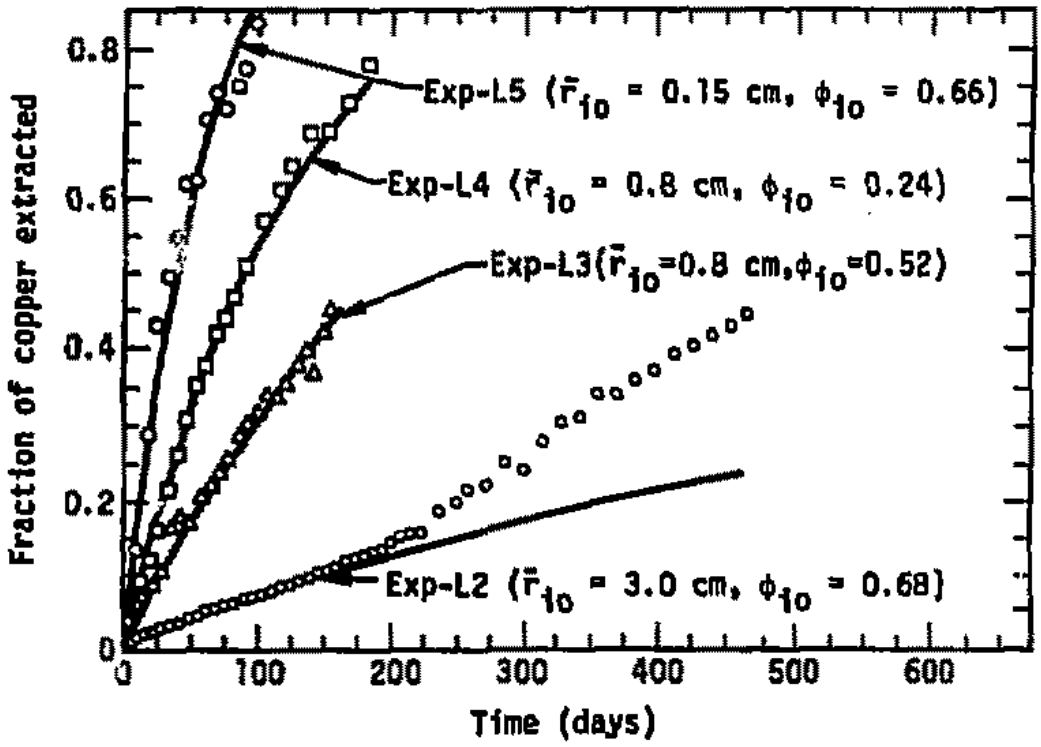

FIG. 9. - Copper Extraction Curves Calculated from Analytically Integrated Rate Equation

then determined empirically using the above values of β' and γ (ϕ_{io} = 0.68, 0.52, 0.24, and 0.66 for Exp-L2, -L3, -L4, and -L5, respectively). These shape factors are consistent with direct measurements of size and projected area of the ore particles.

The agreement between calculated and measured copper recoveries shown in figure 9 was good—except for Exp-L2, which leached faster than predicted. The general agreement, however, serves to identify the kinetic model and provide support for a mixed kinetic system involving surface reaction and pore diffusion control. Extension of the model to handle the actual particle size distribution and to take into account changes occurring during the leaching is most readily accomplished by a numeric integration of the rate Eq. (13) using a finite-difference computer code.

Numeric Integration of Leaching Rate

A finite-time-interval computer code based on a modified form of Eq. (13) was developed. We will first extend the model to handle the actual ore particle size distribution.

The size distribution of the ore particles was described by a tabulated set, $[d_i, Y(d_i)]$, where $Y(d_i)$ is the cumulative weight fraction of ore having a diameter less than d_i. This cumulative

size distribution was then partitioned into a set (r_{io}, W_i), where W_i is the weight fraction of ore having an average radius r_{io}.

The amount of $CuFeS_2$ dissolved from one ore particle of radius r_{io} during time increment Δt_j is given by

$$\Delta n_{ij} = \left(\frac{dn}{dt}\right)_i \Delta t_j . \tag{23}$$

The values of Δt_j used in this numeric integration are sufficiently small to obtain a stable solution that is independent of the choice of Δt_j. The new radius of the unreacted core of this particle is then calculated from the relation

$$\left(r_i^3\right)_{j+1} = \left(r_i^3\right)_j - \frac{3\Delta n_{ij}}{4\pi\rho_r n_o}, \tag{24}$$

where n_o = moles $CuFeS_2$/g ore. The total amount of $CuFeS_2$ dissolved per gram of ore particles of radius r_{io} during time increment Δt_j is given by

$$\Delta n_j = \sum_i \frac{3W_i \Delta n_{ij}}{4\pi r_{io}^3 \rho_r}, \tag{25}$$

The incremental fraction of $CuFeS_2$ dissolved during Δt_j is

$$\Delta\alpha_j = \frac{\Delta n_j}{n_o}, \tag{26}$$

Finally, after each time increment, the total fraction of $CuFeS_2$ dissolved (α) and the time (t) are evaluated.

Before applying Eqs. (23)-(26), we will modify the basic rate expression as given in Eq. (13) to take into account two important phenomena. First, to adequately describe the initial leaching characteristics, consideration must be given to the higher grade of $CuFeS_2$ near the surface of an ore fragment compared to the grade within the fragment. This is a consequence of the nature of preferential ore breakage along planes that are somewhat richer in $CuFeS_2$. The following model was found to adequately describe this phenomenon. For an ore particle of radius r_{io}, let the region of higher grade be equal to that volume of ore contained in an exterior shell of thickness Δr_{io} such that the grade of $CuFeS_2$ in that region

be an arbitrary factor of 2 times the grade in the remainder of the particle. This can be stated mathematically by the equations

$$G = \frac{2G_o}{\left[2 - \left(1 - \frac{\Delta r_{io}}{r_{io}}\right)^3\right]} \qquad \text{for } r_i > (r_{io} - \Delta r_{io}) \tag{27}$$

and

$$G = \frac{G_o}{\left[2 - \left(1 - \frac{\Delta r_{io}}{r_{io}}\right)^3\right]} \qquad \text{for } r_i \leq (r_{io} - \Delta r_{io}), \tag{28}$$

where r_i is the radius of the unleached core and G_o is the average $CuFeS_2$ grade of the whole particle.

If the shell thickness Δr_{io} is expressed as

$$\Delta r_{io} = \mu r_{io}, \tag{29}$$

then the initial leaching rates for all experiments will be shown to be correlated by $\mu = 0.004$. This formulation ascribes a greater enhancement of initial leaching rates for greater particle sizes, which is consistent with the experimental leaching data.

Next, Eq. (13) must be modified to describe the enhanced leaching rates that are observed in later stage leaching, which is particularly evident for Exp-L2 (figure 9). As explained earlier, the enhanced reaction results from the generation of cracks and fissures, which increase the effective reacting interfacial area. The effect is illustrated diagramatically in figure 10, based upon visual examination of ore particles removed from Exp-L2. Pores and fissures develop beyond the reaction interface into the core. The general effect is very complicated, and detailed phenomenological evaluation would be extremely difficult to build into any model. Undoubtedly, variations in porosity and tortuosity occur concurrent with an increase in interfacial area. Also, analysis of the data indicates the effect is greater for larger ore fragments than smaller ones. This is not surprising, since larger particles have more imperfections due to their larger volume. Also, larger particles must be exposed to solution longer than smaller particles for the same extraction.

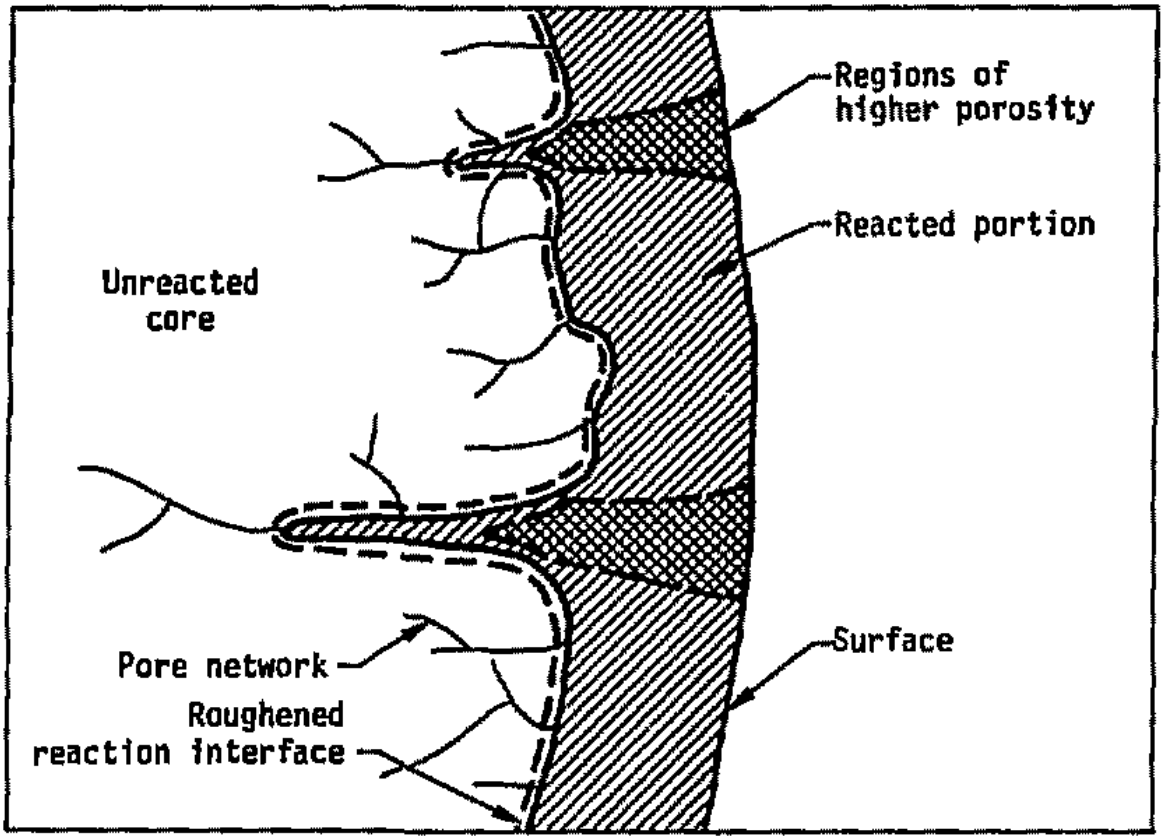

FIG. 10. - Partially Leached Ore Showing Roughening of Reaction Interface Caused by Preferential Leaching Through Mineralized Zones and Imperfections

The model would be more useful if one operating parameter could be described to account for the observed variation in kinetics. To do this we have assumed that regions of deep penetration may be treated as an increase in area for diffusion equal to the increase in area of the reaction zone for the chemically controlled part of the process. This permits a single parameter to operate upon both the chemically and diffusion-controlled processes. This was done by allowing the shape factor (ϕ_i) to vary systematically with r_i, approaching some limiting degree of surface roughness.

It is assumed the change of ϕ_i with r_i is proportional to the interfacial area according to the equation

$$\frac{d\phi_i}{dr_i} = \frac{\lambda r_i^2}{\phi_i}, \tag{30}$$

which gives, for the boundary conditions $r_i = r_{io}$ when $\phi_i = \phi_{io}$,

$$\phi_i = \left[\phi_{io}^2 - \frac{2}{3}\lambda\left(r_{io}^3 - r_i^3\right)\right]^{1/2}. \tag{31}$$

The differential rate expression then becomes

$$\left(\frac{dn}{dt}\right)_i = -\frac{4\pi r_i^2 C_b}{\left[\phi_{io}^2 - \frac{2}{3}\lambda\left(r_{io}^3 - r_i^3\right)\right]^{1/2}} \left[\frac{1}{\left(\frac{1}{G\beta}\right) + \left(\frac{\sigma}{Df}\right)\left(\frac{r_i}{r_{io}}\right)(r_{io} - r_i)}\right]. \quad (32)$$

A lower limit of 0.17 ϕ_{io} was placed on ϕ_i. Smaller values would be difficult to justify, since gross decrepitation of the particle would be expected. This lower limit of ϕ_i is equivalent to a sixfold increase in effective area before a steady-state area configuration is attained.

Copper extraction curves based on Eq. (32) can now be calculated by numerical integration in the procedure described. The value used for the oxygen concentration in the bulk solution (C_b) at 90°C and 400 psi is 2.05×10^{-5} moles cm^{-3} (8). There are four parameters independent of ore particle geometry, namely: β (the chemical rate constant), Df/σ (the diffusion rate constant), μ [the initial rate enhancement parameter in Eq. (29)], and λ (the later rate enhancement parameter). One set of these four parameters was determined to be applicable to all five experiments: $\beta = 4 \times 10^{-6}$ cm sec^{-1}, $Df/\sigma = 2.42 \times 10^{-8}$ cm^2 sec^{-1}, $\mu = 0.004$, and $\lambda = 0.15$. The remaining parameter (ϕ_{io}) is different for each experiment because of difference in ore particle geometry. The shape factor was normalized to $\phi_{io} = 1$ for Exp-L1, in which the ore particles were closest to isometry. The ϕ_{io} values for the remaining four experiments were then empirically determined by trial integration of Eq. (32) ($\phi_{io} = 0.75$, 0.52, 0.26, and 0.70 for Exp-L2, -L3, -L4, and -L5, respectively). The final calculated leaching curves are shown in figure 11 (Curve A) for Exp-L1, figure 12 (Curve A) for Exp-L2, and figure 13 for the other experiments. Calculated leaching curves are also shown in figures 11 and 12 when enhanced leaching rates due to change in ϕ_i are neglected (Curve B) and when both that effect and also the enhanced initial reaction rates due to excess surface chalcopyrite are neglected (Curve C). Neglecting the latter two effects for the smaller ore sizes in figure 13 gave little or no departure from the curves shown for the complete calculation. This is implicit in the model, and it accounts for the lower probability in small ore particles of either having an enrichment of chalcopyrite on their surfaces or developing an increase in interfacial reaction area due to imperfections.

Discussion of Model

The model, as presented, is applicable to calculation of leaching rates at 90°C for a wide range of ore particle sizes. The model adequately describes both the initial leaching rates and the long-term leaching characteristics, even after partial decrepitation of

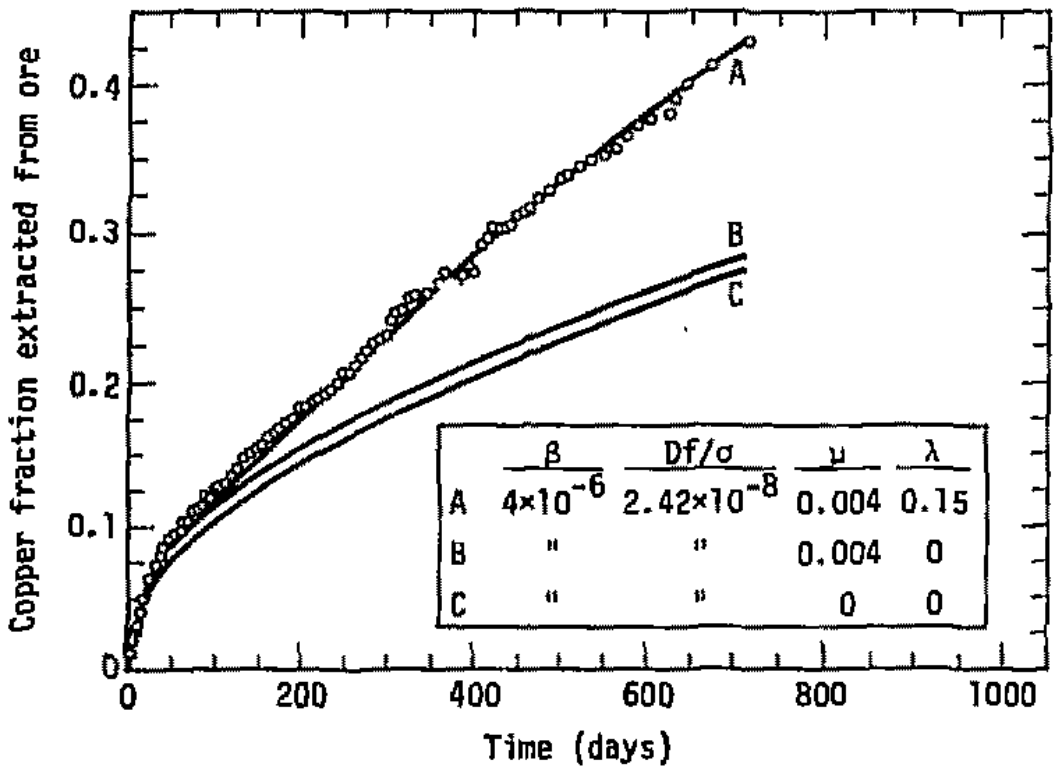

FIG. 11. - Exp-L1 Copper Extraction Curves Calculated by Numerical Integration of Rate Equation

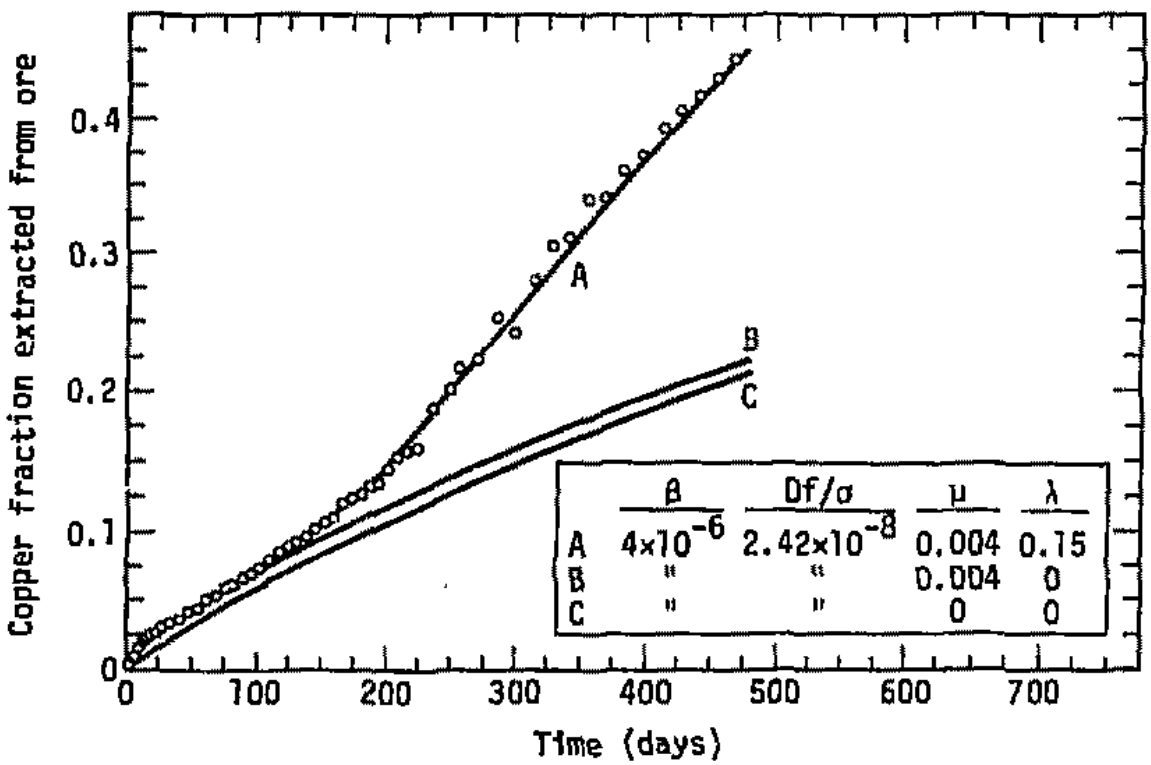

FIG. 12. - Exp-L2 Copper Extraction Curves Calculated by Numerical Integration of Rate Equation

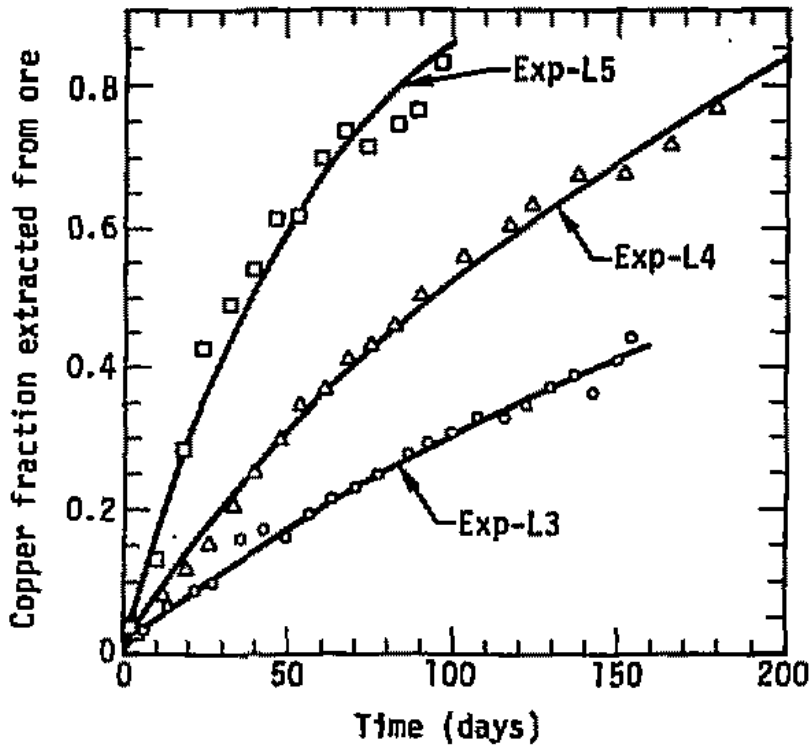

FIG. 13. - Copper Extraction Curves Calculated by Numerical Integration of Rate Equation for Exp-L3, -L4, and -L5

the ore particles. The only parameter that differs in comparing data for the various experiments is ϕ_{lo}. The variations in ϕ_{lo} determined by the preceding numerical analysis are physically real in that the variation in shape factors are clearly evident by physical examination of the ore particles.

It would be desirable to extend the model to apply to temperatures other than 90°C. Insufficient data have been obtained for ore at various temperatures to determine temperature coefficients unambiguously. The difficulty encountered results from changes in both physical and chemical characteristics of the system with temperature, the major problem being the variation in the chemistry and distribution of products of reaction. Much more must be learned about the solution chemistry of the system at various temperatures so that necessary pH adjustment may be made to normalize the physical properties of the system. However, the significance of the constants determined at 90°C may be partially analyzed and the expected effect of temperature on these constants approximated.

Essentially, three quantities are temperature dependent: C_b, β, and Df/a. The temperature dependence of the solubility of oxygen in water (C_b) has been measured (8). The dependence of C_b on temperature and pressure can be summarized from that data by the following Henry constant (moles cm^{-3} psi^{-1}) for T in °C:

$$k_h = 1.068 \times 10^{-7} - 1.168 \times 10^{-9}\, T + 6.109 \times 10^{-12}\, T^2. \qquad (33)$$

Next, it is possible to approximate the temperature dependence of the value of β determined experimentally, since β contains the chemical reaction rate constant and physical constants required by the model. The reaction rate constant k(cm sec^{-1}) is related to the specific rate constant k' (sec^{-1}) by the equation

$$\frac{k\rho_p}{M} = Sk_o k', \qquad (34)$$

where S is the fraction of the surface of $CuFeS_2$ that is chemically active, M is the molecular weight of $CuFeS_2$, and k_o is the total number of moles of surface sites per cm^2 on the surface of $CuFeS_2$. The value of k_o (moles cm^{-2}) may be approximated by

$$k_o = \left(\frac{\rho_p}{M}\right)^{2/3} \left(\frac{1}{N}\right)^{1/3} = 9.55 \times 10^{-10}, \qquad (35)$$

where N = Avogadro's number. From absolute reaction rate theory (9), the specific rate constant k' is given by

$$k' = \frac{k_B T}{h}\, e^{-\frac{\Delta H^{\ddagger}}{RT}}\, e^{\frac{\Delta S^{\ddagger}}{R}}, \qquad (36)$$

where k_B = the Boltzmann constant, h is the Planck constant, $\Delta H^{\ddagger}$ is the enthalpy of activation and $\Delta S^{\ddagger}$ is the entropy of activation. For condensed systems, Eq. (36) may be written in terms of the experimental activation energy ΔE as

$$k' = \frac{ek_B T}{h}\, e^{-\frac{\Delta E}{RT}}\, e^{\frac{\Delta S^{\ddagger}}{R}}. \qquad (37)$$

Also, for the model proposed, the entropy of activation would be expected to be small, containing only vibrational degrees of freedom. Considering $\Delta S^{\ddagger} = 0$, Eq. (14) becomes

$$\beta = \frac{3\rho_r \delta M}{r_p \rho_p^2} Sk_o \frac{ek_B T}{h}\, e^{-\frac{\Delta E}{RT}}. \qquad (38)$$

According to Eq. (38) the ratio $\delta S/d_p$ may now be evaluated as

$$\frac{\delta S}{d_p} = 1.25 \times 10^{-12} e^{\frac{\Delta E}{RT}}, \tag{39}$$

where d_p = copper sulfide particle diameter, $\rho_p = 4.2$ for chalcopyrite, $\rho_r = 2.6$ for the bulk ore, and $\beta = 4 \times 10^{-6}$. It is necessary to estimate reasonable limits on the value of $\delta S/d_p$. Examination of partially leached specimens indicates a sharp reaction interface such that δ/d_p cannot be much greater than 10. The quantity S is the fraction of the cathodic surface of the $CuFeS_2$, which results in the reduction of oxygen. If the anodic and cathodic surfaces are equal in area, S would be 0.5. It seems unlikely that it would be less than 0.1. Using the limits $1 < \delta/d_p < 10$ and $0.1 < S < 1$, the range of values for $\delta S/d_p$ would be $0.1 < \delta S/d_p < 10$. This gives a range of 18.0 to 21.4 kcal/mole for the value of ΔE. This is in agreement with values previously reported (2,10,11) and lends strong support to the validity of the proposed model.

Finally, we consider the quantity Df/σ. The molecular diffusivity of oxygen in water (D) is 2.5×10^{-5} cm^2 sec^{-1} at 25°C (12). Although D is proportional to the ratio of absolute temperature to viscosity in dilute solution at 1 atm (13), the actual value of D has not been measured—nor can it be reliably calculated—for the conditions of interest here (90°C, 27 atm, and solutions of relatively high ionic strength). However, the overall temperature dependence of D is indeed small compared with that of the chemical reaction rate constant β, and it can therefore be reasonably neglected. Thus, the principal temperature, dependent parameters have now been included in the model.

Further consideration of the quantity Df/σ allows certain other physical features of the ore to be addressed. The value of $f = 0.0109$ can be calculated using the experimental value of $Df/\sigma = 2.42 \times 10^{-8}$ cm^2 sec^{-1}, together with $D = 2.5 \times 10^{-5}$ cm^2 sec^{-1} and $\sigma = 11.25$ [Eq. (7)]. The quantity f can also be expressed as

$$f = \frac{f'}{\tau}, \tag{40}$$

where f' is the effective pore area perpendicular to the direction of diffusion and τ is the tortuosity. Calculation of f' from the measured porosity of the sample and the volume fraction of contained chalcopyrite then will allow an estimation of τ in the following way. If ϕ is the porosity, then $\phi/3$ is the effective porosity in the direction of diffusion. The effective pore area perpendicular to the direction of diffusion is then

$$f' = \left(\frac{\phi}{3}\right)^{2/3} \phi, \tag{41}$$

where Φ is the probability that a chalcopyrite particle is in the diffusion path. This probability is related to the effective cross-sectional area of total mineral and total porosity within a unit of volume,

$$\Phi = \left(\frac{G\rho_r}{\rho_p \phi}\right)^{2/3} . \qquad (42)$$

Combining Eqs. (41) and (42) gives

$$f' = \left(\frac{G\rho_r}{3\rho_p}\right)^{2/3} \qquad (43)$$

The value of f' according to Eq. (43) is 0.026 and is independent of ϕ, which is true only if the mineral is essentially contained within the pore network of the mineral. The calculated tortuosity according to Eq. (40) is thus 2.38. This reasonable result illustrates the consistency of the proposed leaching model in terms of related physical features of the ore.

Mixed Kinetics

It is possible to determine the relative importance of diffusion and chemical reaction in the mixed kinetic model. For Exp-L1, diffusion becomes the predominant rate-controlling factor after approximately 32 percent reaction at 90°C. The implications are interesting in that for high degrees of extraction, the rate will be controlled by the physical features of the rock and essentially independent of the sulfide mineral types. For a given ore geometry and physical make-up, the rational reaction rate will be the same for all copper sulfide minerals during the final ($\alpha > 0.5$) stage of leaching. The true rate would be modified by the stoichiometry factor σ and the variable effect of deposited salts. Sulfides requiring less oxygen for an equivalent copper release would leach faster, since the kinetics are related to oxygen diffusion. During the early stages of leaching ($\alpha < 0.5$), the rate of release of copper will be greatly dependent upon the sulfide mineral type.

Comparison With Other Leaching Models

The earlier model of Lewis and Braun (2) for calculating leaching rates was based on the measured chemical rate constant for oxidation of chalcopyrite and on diffusion limitations that were introduced by means of an exponential decrease of oxygen concentration as a function of distance into the ore particle empirically determined by preliminary ore leaching data. The present model is a more rigorous treatment of the mixed kinetics, giving a better estimate of the relative importance of chemical reaction and diffusion.

A recent model has been proposed by Bartlett (14) to describe ore leaching, based on the continuity equation for oxygen within an ore particle. His calculated leaching curve agreed with the data of Exp-L1 (Bartlett's figures 5 and 6) only if the following changes in rock porosity are invoked: the porosity, starting at 0.05, must first decrease to 0.03 at 100 days and then gradually increase thereafter, reaching 0.05 at 2 years. Such porosity changes, in leaching ore at 90°C and pH 1.9, have not been observed. Rather, the measured porosity remains at nearly 0.06 during leaching under these conditions. In addition, Bartlett's model does not treat two important phenomena: enhanced initial leaching rates due to relative enrichment of chalcopyrite near the ore surface and enhanced leaching rates due to increasing interfacial reaction zone area in long-term leaching. Our present model addresses both of these phenomena in a physically realistic way.

SUMMARY AND CONCLUSIONS

The mixed kinetic model proposed has shown excellent agreement for laboratory leaching results for the ore type investigated. The model accounts well for such physical features as density and porosity and contains kinetic parameters that may be extrapolated to such ambient conditions as pressure and temperature. As a first approximation, observed mineralogical make-up, both chemical and physical, can be related to expected kinetic results. The following are specific conclusions related to the San Manuel ore used:

(1) The rate of reaction is controlled by the rate oxygen diffuses to, and reacts with, sulfide minerals within the ore fragment.

(2) The reaction zone of the order of a few sulfide particles in diameter moves through the ore fragment, accounting for a systematic decrease in kinetics.

(3) Increased rates resulting from random penetration along fracture planes or planes of mineralization are treated successfully by the model.

(4) Measured kinetic parameters may be directly related to physical factors such as pore volume, ore density, mineral density, tortuosity and surface roughness.

(5) Predictions regarding the effect of temperature may be made, since chemical and diffusional reaction rate constants are included.

(6) Results for sized-particle tests may be applied directly to mixed-particle distributions by means of the proposed model.

ACKNOWLEDGMENT

The authors gratefully acknowledge the dedicated efforts of H. Gates and D. Wooster in the experimental work, the technical contributions of other LLL personnel, and the donation of 50 tons of San Manuel ore by the Magma Copper Corporation.

REFERENCES

1. Lewis, A. E., "Chemical Mining of Primary Copper Ores by Use of Nuclear Technology," in Proceedings of Symposium on Engineering with Nuclear Explosives," Amer. Nucl. Soc., CONF-700101, Vol. II, 1970.

2. Lewis, A. E., and R. L. Braun, "Nuclear Chemical Mining of Primary Copper Sulfides," Lawrence Livermore Laboratory, Rept. UCRL-73284, 1972, presented at the 1972 AIME Meeting, San Francisco, Calif.

3. Lewis, A. E., R. L. Braun, C. J. Sisemore, and R. G. Mallon, "Nuclear Solution Mining—Breaking and Leaching Considerations," Lawrence Livermore Laboratory, Rept. UCRL-75080, 1973, to be presented at the 1974 AIME Mtg., Dallas, Tex.

4. Potter, G. M., U.S. Bureau of Mines, Salt Lake City, private communication, Dec. 7, 1972.

5. Harris, J. A., "Development of a Theoretical Approach to the Heap Leaching of Copper Sulfide Ores," Proc. Aust. Inst. Min. Met., 230, 1969, p. 81.

6. Valensi, G., "Cinétique de l'oxydation de sphérules et de poudres métalliques," Comptes Rendes, 202, 1936, p. 309.

7. Strangway, P. K., H. O. Lien, and H. U. Ross, "Studies on Kinetics of Iron Oxide Reduction," Can Met. Quart., 8, 1969, p. 235.

8. Zoss, L. M., S. N. Suciv, and W. L. Sibbitt, "The Solubility of Oxygen in Water," Trans. Amer. Soc. Mech. Engrs., 76, 1954, p. 69.

9. Glasstone, S., K. J. Laidler, and H. Eyring, The Theory of Rate Processes, McGraw-Hill, New York, 1941, p. 196.

10. Warren, I. H., "A Study of the Pressure Leaching of Chalcopyrite, Chalcocite, and Covellite," Aust. J. Appl. Sci., 9, 1958, p. 36.

11. Dutrizac, J. E., R. J. C. McDonald, T. R. Ingraham, "The Kinetics of Dissolution of Synthetic Chalcopyrite in Aqueous Acidic Ferric Sulfate Solutions," Trans TMS-AIME, 245, 1964, p. 955.

12. Perry, J. H., Chemical Engineer's Handbook, 4th Ed., R. H. Perry, C. H. Chilton, and S. D. Kirkpatrick, Eds., McGraw-Hill, New York, 1963, pp. 14-26.

13. Wilke, C. R., and P. Chang, "Correlation of Diffusion Coefficients in Dilute Solutions," J. Am. Inst. Chem. Engrs., 1, 1955, p. 264.

14. Bartlett, R. W., "A Combined Pore Diffusion and Chalcopyrite Dissolution Kinetics Model for In Situ Leaching of a Fragmented Copper Porphyry," in Proc. Int'l. Symp. Hydrometallurgy, AIME New York, 1973.